The Simulation of Elastic-Plastic Flows with Fracture in Target at Intense Irradiation[1]

A.P. Yalovets, N.B. Volkov*, A.E. Mayer, A.B. Markov**, and V.P. Rotshtein**

South-Ural State University, Lenina prospect, 76, Chelyabinsk, 454080, Russia, +7(351)267-91-40, .yal@csu.ru
**Institute of Electrophysics, Russian Academy of Sciences, Ural Branch, Amundsena street, Ekaterinburg, 620016, Russia*
***Institute of High-Current Electronics, Russian Academy of Sciences, Siberian Branch, 2/3, Akademicheskii prospect, Tomsk, 634055, Russia*

Abstract – The numerical simulation results of the rear surface spallation of copper targets irradiated with a relativistic high-current electron beam are presented here. The simulations were done in 2D cylindrical formulation using BETAIN2 code [1]. The phenomenological model [2, 3] was used to take fracture into account. This model describes the kinetics of micro-pores under the action of strains and stresses. The irradiation of metal targets by SINUS-7 accelerator was simulated in the present paper, a spallation of copper targets was early obtained experimentally [4] at this facility. There is accordance between the present simulations and experiments [4] in the next aspects: the dependence of spalled layer depth versus the target thickness; the maximal thickness of the target with the spallation traces; the common character of spallation. The spalled layer depth increases nonlinearly with the target thickness increase. The two-dimensionality of the target deformations causes additional strains fracturing the target, and so it plays an important role in spallation. The corresponding 1D simulation does not indicate the spalltion at all.

1. Introduction

The heat and strain processes induced in materials by pulsed power irradiation, particularly with intense pulsed electron beams, result in various types of structure and property modification. These modifications can be positive in terms of the increase of surface quality and strength of the irradiated samples. They can be negative for technological applications as well: the formation of micro-craters, the distraction (spallation) of target.

The non-destructive beams are usually used for technological goals. However the investigations of more intense energy fluxes interaction with matter are under the great interest. This interaction can generate the powerful stress waves, which are able to spall the target after the reflection from rear surface. The investigations of spall fracture at high strain rates are impotent in the physics of fast phenomena.

The spallation of copper specimens by SINUS-7 accelerator was experimentally investigated in [4]. The results of numerical simulations of those experiments are discussed here. The model of fracture and the set of its constants, previously applied for the high-speed impacts simulation [5], were used. The obtained accordance of calculative and experimental data lets one conclude the applicability of this model of fracture for the description of metal targets spallation under the action of the relativistic high-current electron beam.

2. Mathematical model

The 2D numerical code BETAIN2 [1], modified for the fracture accounting, was used for simulations. This code was constructed for the description of intense electron beam interaction with matter and solves the equations system, comprising the kinetic equation for the fast particles of beam and the equations of the mechanics of continua. The next models are used for substance dynamics: elastic-plastic model in solid and hydrodynamic one in non-solid parts of the target. The mechanics of continua equations system has the form:

a) the equation of motion

$$\rho \dot{v}^{(r)} = \frac{\partial \sigma_{rr}}{\partial r} + \frac{\partial \sigma_{rz}}{\partial z} + \frac{S_{rr} - S_{\varphi\varphi}}{r}, \qquad (1)$$

$$\rho \dot{v}^{(z)} = \frac{\partial \sigma_{zz}}{\partial z} + \frac{\partial \sigma_{rz}}{\partial r} + \frac{S_{zr}}{r}, \qquad (2)$$

here $\sigma_{ik}=-P\delta_{ik}+S_{ik}$ are the components of stress tensor, P – the pressure, S_{ik} – the deviators of stresses, $(v^{(z)},v^{(z)})$ – the velocity, ρ – the density;

b) the equation of continuity

$$\frac{\dot{V}}{V} = \frac{\partial v^{(r)}}{\partial r} + \frac{v^{(r)}}{r} + \frac{\partial v^{(z)}}{\partial z}, \qquad (3)$$

here V is the specific volume;

c) the equation for specific internal energy U (the energy conservation law)

[1] This work was partially financially supported by the Presidium of the Ural Branch of the Russian Academy of Science in the frames of the special program of interdisciplinary researches, realized jointly by the scientists of the Ural, the Siberian, and the Far-Eastern Branches of the Russian Academy of Science. This work was also partially financially supported by the "Human Capital Foundation".

$$\rho\dot{U} = (S_{zz}v_{zz} + S_{rr}v_{rr} + S_{\varphi\varphi}v_{\varphi\varphi} + 2S_{rz}v_{rz}) - \\ -P\frac{\dot{V}}{V} + \nabla(\kappa\nabla T) + D, \quad (4)$$

here D – the energy-release function, accounting the target heating by beam, T – the temperature, $\kappa=\kappa(\rho,T)$ – the coefficient of heat conductivity[6], v_{ij} – the strain rates tensor;

d) the equation of state (5) for the pressure, the Hooke's law (6) and the Mizes's condition of yield (7) for the deviators of stresses

$$P = P_{EOS}(\rho,U), \quad (5)$$

$$\dot{S}_{rr} = 2\mu\left(\frac{\partial v^{(r)}}{\partial r} - \frac{1}{3}\frac{\dot{V}}{V}\right) + \dot{\delta}_{rr},$$
$$\dot{S}_{zz} = 2\mu\left(\frac{\partial v^{(z)}}{\partial z} - \frac{1}{3}\frac{\dot{V}}{V}\right) + \dot{\delta}_{zz},$$
$$\dot{S}_{\varphi\varphi} = 2\mu\left(\frac{v^{(r)}}{r} - \frac{1}{3}\frac{\dot{V}}{V}\right), \quad (6)$$
$$\dot{S}_{rz} = \mu\left(\frac{\partial v^{(r)}}{\partial z} + \frac{\partial v^{(z)}}{\partial r}\right) + \dot{\delta}_{rz},$$

$$S_{rr}^2 + S_{\varphi\varphi}^2 + S_{zz}^2 + 2S_{rz}^2 \le \frac{2}{3}Y^{(0)}, \quad (7)$$

here $Y^{(0)}$ is the yield stress, δ_{ik} are the corrections, accounting a rotation by the substance deformations [7].

The dynamical values of yield stress and share modulus [5] were used in the present work. We set μ=0 in the non-solid parts of target. The mechanics of continua equations system is solved numerically in BETAIN2 by the method, described in [8].

The equations system (1–7) is completed by the kinetic equation for electrons

$$\hat{\mathrm{L}}\,\Psi(z,\Omega,T^{(b)}) = S; \quad (8)$$

here $\Psi(z,\Omega,T^{(b)})$ is the flux density of particles differential in angle and energy, S – the source function, $\hat{\mathrm{L}}$ – the translation operator. The dose rate (the energy-release function) is determined as the next

$$D(z,t) = \int d\Omega \int dT^{(b)} B(T^{(b)})\Psi(z,\Omega,T^{(b)}), \quad (9)$$

here $B(T^{(b)})$ is the specific loose of energy. The electron transfer model accounts the elastic scattering, the fluctuations of loose of energy in inelastic collisions, and the creation of secondary electrons. The used in BETAIN2 numerical solution of the electron transfer problem is described in [9].

The model of fracture [2, 3] is used for accounting of target spallation. The damageable substance is characterized by the presence of micro-cavities (micro-pores and micro-cracks). The whole volume of substance V is composed by the condensed (infact) phase with density ρ_c, filling the volume V_c, and by the micro-cavities with zero density, filling the volume V_f. The pressure is $P_c=P_{EOS}(\rho_c,U)$ in the condensed phase. The average density and average pressure, appeared in system (1–7), are determined by the relations: $\rho=\rho_c(V_c/V)$, $P=P_c(V_c/V)$. To simulate the substance dynamics with fracture it is necessary to add the following equation of the micro-cavities specific volume evolution to the mechanics of continua equations system (1–7):

$$\dot{V}_f = \begin{cases} -sign(P_c)K_f(|P_c| - P^*)(V_2 + V_f), \\ \quad if \quad P_c < P^* \quad or \\ \quad (P_c > P^*, V_f > 0); \\ 0, \quad otherwise; \end{cases} \quad (10)$$

here $P^*=P_kV_1/(V_f+V_1)$; V_1, V_2, P_k, K_f – the set of the constants, experimentally determined for each substance. The set of constants from [5] was used in the present paper.

The active-type kinetic model of fracture is used here, which accounting the uninterrupted change of substance properties due to the micro-cavities grow; the variations of yield stress and share modulus are accounted in particular. This model of fracture was included in 2D code BETAIN2.

3. Simulations and discussion

The simulations were done on the Lagrangian computational grid with a dimension varied from 120×100 up to 120×300 meshes depending on the target thickness. The target was treated as two subregions. The first subregion presents the beam particles energy-release zone with the thickness of 1mm, a wide-range equation of state [10] was used here. The second subregion is a residual part of the target with the depth varied from 1mm up to 5 mm, a Mi-Grunaizen equation of state was used in the second subregion. A radius of computational region was equal to 10mm. The radial distribution of current density was set according to the normal law with maximal radius of the irradiation zone equal to 8 mm. The current and voltage oscillograms were taken from [4]: the pulse duration is 50 ns, the maximal energy of the electrons is 1.3 MeV, and the maximal current of the beam is 17 kA.

The calculated density distributions (a) at the time moment 4 s are presented on Fig. 1 and 2 for the targets with 2 mm and 4 mm thickness respectively. The dark regions correspond to the substance with the solid density, the light regions correspond to the cavities with zero density and the gray regions correspond to the dense plasma or to the destructed arrears of target. The photographs of the pieces of irradiated targets from [4] are printed in scale on these figures as well for the comparison.

One can see a formation of erosion zone at the front surface of target on the calculated distributions (Fig. 1, 2). This erosion was caused by substance melting, the evaporation and expanding of plasma layer. The erosion zone radius is close to beam radius. Nearer to the edge of irradiated zone the melting

and evaporation take place only inside the target (at the depth of the energy-release function maximum); and here the surface layer, remaining in condensed state, are bending hack by the expanding plasma.

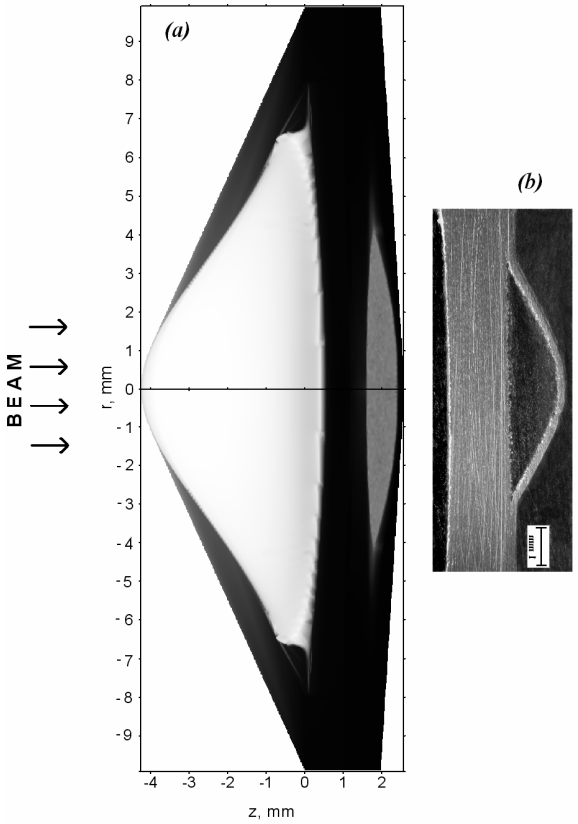

Fig. 1. The simulated density distribution (a) and the experimental [4] cross section (b) of 2 mm Cu target

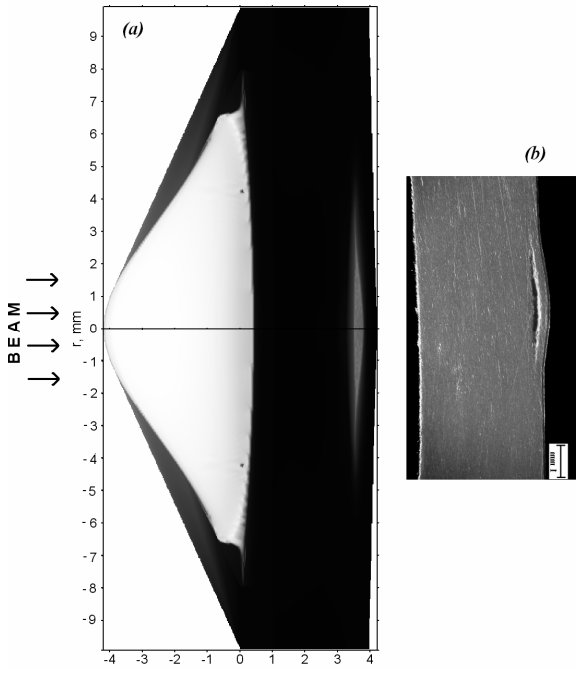

Fig. 2. The simulated density distribution (a) and the experimental [4] cross section (b) of 4 mm Cu target

A spallation observed at the rear surface of target in 2D simulations as well as in experiments [4]. An intense heating of substance in energy-release zone and a recoil pulse from expanding plasma generate shock wave with the amplitude of stresses exceeded 10 GPa. The spallation is initiated by the stretching stresses, originating due to the shock wave reflection from rear target surface. The comparability of beam radius with the depth of energy-release zone as well as with the thicknesses of the targets determines an important role of the two-dimensionality of the target deformations. The corresponding one-dimensional simulations do not indicate spallation: there was a growth of total micro-cavities volume near the rear surface of target but there was not a fracture. One can conclude from this fact that the radial distribution of the beam current density and the finiteness of the beam cross-section strongly influence on the spallation. The mentioned factors lead to the more complicated pattern of stress waves and to the larger peak values of stresses (on the beam axis) in comparison with 1D (the broad and uniform beam) case. Furthermore, the recoil pulse of plasma expansion substantially bends the target (see Fig. 1, 2), this bending generates additional stretching stresses at the rear surface of target. Thus, the appropriate numerical simulations of the spallation of target irradiated with the relativistic high-current electron beam are able only in 2D formulation at least.

There is a destruction area between the spalled layer and the main part of the target; the inclusion volume fraction of defects (micro-cavities) reaches the tens of the percents in the destruction area. Here an average density of substance is substantially lower than the solid-phase value (it is seen as a grey zone near the rear surface of target on Fig. 1, 2).

There is a weak spallation (the narrow destruction area) in the simulations with the 5 mm thick copper target. There is not spallation but only the accumulation of defects near the rear surface in the simulations with 6mm thick target. These results are in accordance with experimental data [4].

The simulated (curve 1) and experimental [4] (dots 2) dependences of the spalled layer depth versus the thickness of the irradiated copper target are presented on Fig. 3. There is an inaccuracy of the spallad layer depth definition in the simulations connected with numerical discretization (the computational mesh size is equal to 0.02 mm); this inaccuracy is also plotted on Fig. 3.

One can see that the character of calculated dependence $d(l)$ is in a good agreement with experimental data [4]. But there is an excess of the simulated spalled layer depth for thick targets. A possible reason of this deviation can be the difference between the real radial distribution of beam current density and the normal law, used in simulations.

One should emphasize the nonlinear character of the dependence $d(l)$. It was supposed in [4] that this dependence should be linear, as it was in the case of

laser-driven spallation [11, 12]. The simulated electron-driven dependence is really close to the linear at the small target thicknesses (l<2.5 mm) and at the large target thicknesses (l>4 mm). But there is a nonlinear transition between two linear regimes in the range of the average target thicknesses (2.5 mm<l<4 mm). The scale of such transition thicknesses is determined by the beam radius (about 8 mm) and, therefore, by the radius of spalled layer (less than 4 mm). One can conclude that the nonlinear character of the dependence $d(l)$ is a consequence of the two-dimensionality of the spallation process. This nonlinearity does probably not indicate itself in laser-driven spallation [11, 12] due to the substantially smaller thicknesses of spalled targets.

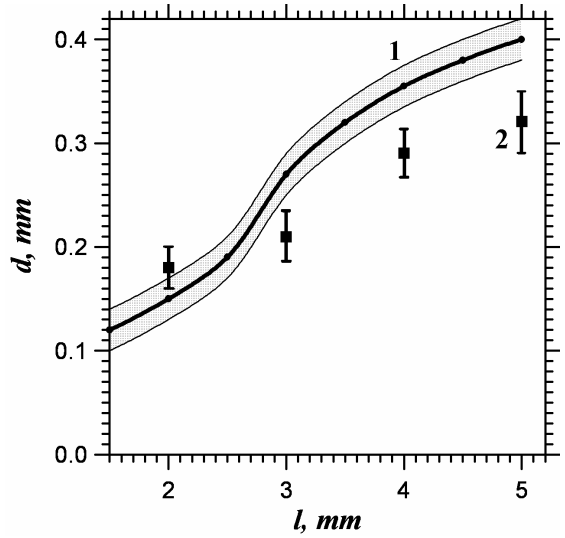

Fig. 3. The depth of spalled layer (d) versus the thickness of the target (l). 1 – simulations, 2 – experimental [4] results

4. Conclusions

The copper target spallation driven by the relativistic high-current electron beam of the SINUS-7 facility was simulated with the use of BETAIN2 numerical code, modified for the fracture accounting. The numerical results are in an agreement with the experimental data [4].

The spallation driven by the intense electron beam is distinctly two-dimensional in its nature, and it can not be described in the one-dimensional formulation.

The dependence of the spalled layer depth versus the thickness of the irradiated target is clearly nonlinear. The nonlinearity is caused by the comparability of the beam and spalled layer radii with the depths of targets, at witch the spallation, driven by the intense electron irradiation, is observed.

References

[1] A.P. Yalovets and A.E. Mayer. *in Proc. 6th Int. Conf. on Modification of Materials with Particle Beams and Plasma Flows*, 2002, pp. 297–299.

[2] G.I. Kanel' and V.V. Scherban', Fiz. Goren. i Vzriva 16 (4), 93 (1980)

[3] G.I. Kanel', V.E. Fortov, A.L. Ni, and V.G. Stel'mah, Fiz. Goren. i Vzriva 19 (2), 121 (1983)

[4] A. B. Markov, S.A. Kitsanov, S.D. Korovin, et. al., *in Proc. 7th Int. Conf. on Modification of Materials with Particle Beams and Plasma Flows*, 2004, pp. 128–133.

[5] S.A. Zelepugin, Thesis for a Doctor's degree in Physics and Mathematics, Tomsk, 2003

[6] N.B. Volkov and A.Z. Nemirovsky, J. Phys. D Appl. Phys, 24, 693 (1991)

[7] M.L. Wilkins, *The simulation of elastic-plastic flows. // Numerical methods in hydrodynamics. Edited by B. Older, S. Fernbah, M. Rotenberg*, Moscow, Mir, 1967.

[8] A.P. Yalovets, Prikl. Mekh. Tehn. Fiz. (1), 151 (1997)

[9] V.V. Valchuk, S.V. Khalikov, and A.P. Yalovets, Mat. Model. 4 (10), 111 (1992)

[10] S.N. Kolgatin and A.V. Khachatur'yants, Teplofiz. Vys. Temp. 20 (3), 90 (1982)

[11] S. Eliezer and I. Gilath, *J. Appl. Phys*, 67 (2), 715 (1990)

[12] M. Boustie and F. Cottet, *J. Appl. Phys*, 69 (11), 7533 (1991)